

Acid-Catalyzed Solvolysis of Softwood in Caprylyl Glycol to Produce Lignin Derivatives

Tomohiro Yamada, Yuki Tobimatsu, Thi Thi Nge, Yusuke Matsumoto, and Tatsuhiko Yamada*



Cite This: *ACS Omega* 2024, 9, 27610–27617



Read Online

ACCESS |



Metrics & More

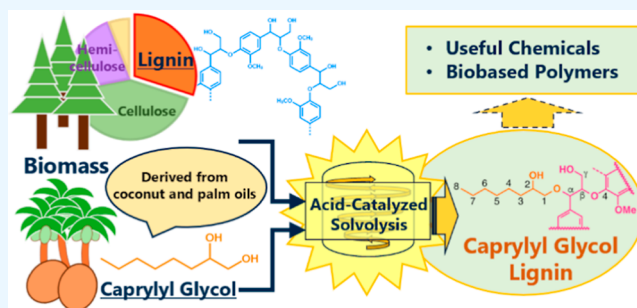


Article Recommendations



Supporting Information

ABSTRACT: Glycol lignin (GL) is produced via the acid-catalyzed solvolysis of softwood meal using glycols such as polyethylene glycol. The physicochemical and thermal properties of GL are expected to be controllable by varying the glycol type. In this study, caprylyl glycol (CG), which is a biobased glycol derived from the caprylic acid component of coconut and palm oils, was used to investigate the effects on the acid-catalyzed solvolysis of softwood. The reactions were performed at 140, 150, and 160 °C for 30–120 min to obtain lignin derivatives (CG-lignin: CGL). The chemical and physical properties of CGLs were investigated. Two-dimensional heteronuclear single-quantum coherence nuclear magnetic resonance analysis suggested that CGL possesses an α -CG- β -O-4 structure as CG is grafted onto the lignin structure. CGLs prepared at higher reaction temperatures exhibited lower molecular weights. The thermomechanical analysis of CGL revealed a glass transition temperature of 89–96 °C and a viscous thermal flow temperature of 134–155 °C.



INTRODUCTION

Lignin exists as a part of the cell walls of vascular plants and is the most abundant natural phenolic polymer on earth.¹ Lignin-derived materials, such as kraft lignin, soda lignin, and lignosulfonates, are obtained as the byproducts of the pulping process. In the kraft pulping process, kraft lignin-dissolved black liquor is incinerated in the recovery process of pulping chemicals to supply energy.¹ Kraft lignin can be used as a solid biofuel, resin, dispersant, adhesive, etc. However, its application in the production of high value-added functional materials remains limited, mainly because of its heterogeneous and condensed lignin structure, sulfur content, and low reactivity and solubility.² An alternative to kraft pulping is organosolv, which is a sulfur-free pulping process.³ A wide variety of organic solvents, including low-boiling (ethanol, methanol, butanol, propanol, and aqueous mixtures of acetone)^{4,5} and high-boiling (ethylene glycol, phenol, and 1,4-butanediol)^{6–8} solvents, have been investigated for organosolv processes. An advantage of using high-boiling-pressure solvents is that the organosolv process can be conducted at atmospheric pressure. Glycol lignin (GL) is produced via the acid-catalyzed solvolysis of softwood meal using high-boiling glycols such as polyethylene glycol (PEG). The acid-catalyzed solvolysis of softwood using a PEG reagent results in the production of PEG-modified lignin derivatives, in which the PEG chains introduced into the lignin structure enable the viscous thermal flow properties of GL.^{9,10} Based on this property, a variety of products, such as glass-fiber-reinforced plastics and carbon-fiber-reinforced plastics, which comprise

GL as a part of the FRP matrix resin, have been developed.¹¹ The physicochemical and thermal properties of PEG-modified GL depend on the size distribution of the source wood meal and the molecular mass of PEG used for the solvolysis process.¹⁰ Furthermore, the aforementioned properties of GL can be manipulated by varying the type of solvolysis reagents other than PEG. In our previous study, poly(ethylene glycol) monomethyl ether (MPEG) was used to produce lignin derivatives (MPEG-lignin). Notably, the molecular weight of MPEG-lignin was lower than that of the GL produced via PEG solvolysis under the same solvolysis conditions (140 °C; 90 min).¹²

In this study, caprylyl glycol (CG), i.e., 1,2-octanediol derived from caprylic acid, which is a component of coconut and palm oils, was used as a solvolysis reagent for GL production. CG can retain the moisture content of human skin upon application, and it exhibits antibacterial functions.^{13,14} Recently, Symrise, a food and personal care ingredient maker, has launched the production of biobased CG.¹⁵ CG contains two hydroxyl groups at the C₁ and C₂ positions, and the alkyl chain extends to one side, which differs from the PEG and

Received: April 5, 2024

Revised: May 31, 2024

Accepted: June 4, 2024

Published: June 10, 2024



MPEG structures used in previous studies. Herein, CG was used to investigate the effects on the acid-catalyzed solvolysis of softwood. The physicochemical and thermal properties of lignin derivatives (CG-lignin: CGL) were investigated via Fourier transform infrared (FTIR) spectroscopy, two-dimensional heteronuclear single-quantum coherence (2D HSQC) nuclear magnetic resonance (NMR) spectroscopy, size exclusion chromatography (SEC), thermomechanical analysis (TMA), and thermogravimetric analysis (TGA).

EXPERIMENTAL SECTION

Preparation of CGL. Figure 1 depicts a schematic of the CGL preparation. The solvolysis reagent was prepared by

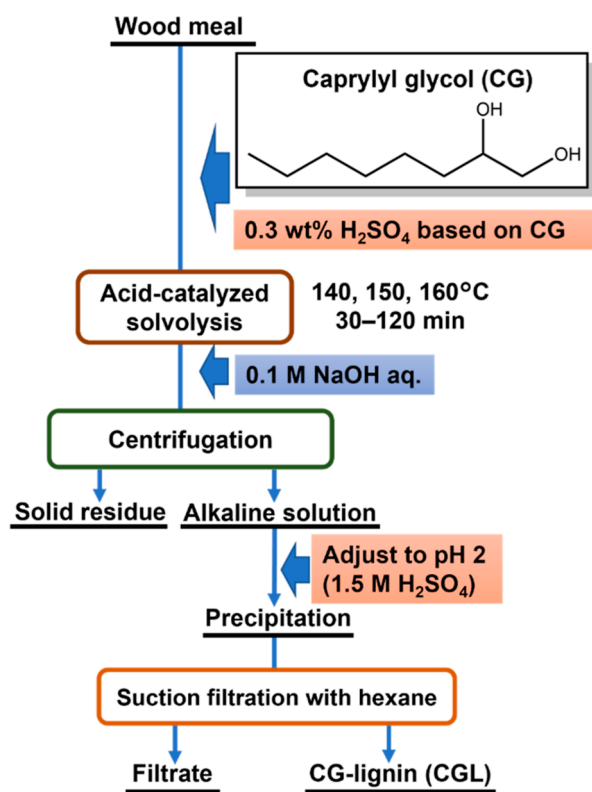


Figure 1. Schematic of the CGL preparation.

adding concentrated sulfuric acid (0.3 wt % of the total amount of the solvolysis reagent) to CG (Tokyo Chemical Industrial Co., Ltd., Tokyo, Japan). Acid-catalyzed solvolysis was conducted as described in our previous paper.¹² The oven-dried (105 °C) softwood Japanese cedar meal (*Cryptomeria japonica*, average particle size distribution = 0.4 mm; 1 g) and solvolysis reagent (5 g) were loaded in a 20 mL test tube reaction vessel. Thereafter, the reaction vessel equipped with a mechanical stirrer was immersed in a preheated oil bath to initiate the reaction. Acid-catalyzed solvolysis was performed at 140, 150, and 160 °C for 30–120 min at atmospheric pressure. Thereafter, the reaction vessel was immersed in an ice-water bath to quench the reaction. The solvolysis products were extracted with 0.1 M NaOH aqueous solution, followed by centrifugation at 3300 rpm for 20 min to separate the solid residues and alkaline solution. The alkaline solution separated into two phases when it stood for a certain period; however, the entire solution was used for the precipitation process.

CGL was precipitated from the alkaline solution using 1.5 M H₂SO₄ by adjusting to pH 2 with stirring. The precipitated CGL was collected via suction filtration by using the following procedure. A 0.2 μm pore size membrane filter was set in a glass filter assembly with a funnel, and hexane (100 mL) was poured into the funnel. Thereafter, the pH-adjusted solution with precipitated CGL was poured into the funnel. CGL was recovered via suction filtration and washed with distilled water, followed by air drying at 25 °C and subsequent vacuum drying at room temperature (25 ± 3 °C) to obtain the recovered CGL as a fine powder.

The yields of fractional components (CGL and solid residue) were calculated on a dry wood basis (eq 1).

Fractional components (%)

$$= [\text{obtained products (g)}/\text{wood meal (g)}] \times 100 \quad (1)$$

The Klason lignin analysis of CGL was performed according to standard NREL procedures¹⁶ with minor modifications¹⁰ as previously described.¹²

Chemical Structure of CGL. The chemical structure of CGL was investigated by using attenuated total reflection (ATR)-FTIR spectroscopy and 2D HSQC NMR analysis. Milled wood lignin (MWL) extracted from Japanese cedar wood meal¹⁷ was used for comparison in these analyses of CGL.

The ATR-FTIR spectra of CGL and CG were recorded using a Nicolet iS50 FTIR spectrometer (Thermo Fisher Scientific, Madison, WI, USA) equipped with a single-crystal diamond top plate ATR accessory. Spectra were collected over the range of 4000–400 cm⁻¹ with an accumulation of 32 scans and a resolution of 4 cm⁻¹. The band intensity of aromatic skeletal vibrations (aromatic ring C=C–C stretching) at 1512 cm⁻¹ was used as an internal reference to normalize all of the CGL spectra after the ATR correction and baseline adjustment.

The 2D HSQC NMR measurements of CGL were performed as demonstrated in a previous study on PEG-lignin production.¹⁰ For NMR analysis, a vacuum-dried CGL sample (approximately 15 mg) was dissolved in dimethyl sulfoxide (DMSO)-*d*₆ (600 μL). A Bruker Biospin AVANCE III 800US spectrometer fitted with a cryogenically cooled 5 mm TCI gradient probe was used to record the 2D HSQC NMR spectra. Adiabatic 2D ¹H–¹³C short-range correlation (HSQC) experiments were performed using the standard Bruker implementation (“hscqctgppsp.3”) using the parameters described by Mandfield et al.¹⁸ Data processing was performed using Bruker TopSpin software, and the central DMSO solvent peaks (δ_C/δ_H: 39.5/2.49 ppm) were employed as the internal references. HSQC plots were obtained with typical matched Gaussian apodization in F2 and squared cosine-bell apodization and one level of linear prediction (16 coefficients) in F1. For contour integration analysis, well-resolved C–H contours from I (β-O-4), II (β-5), III (β-β), OMe, and CG₈ contours were integrated.

SEC Analysis. SEC was performed using a Shimadzu Prominence LC-20AD (Shimadzu Corporation, Kyoto, Japan) system equipped with an ultraviolet (280 nm) and refractive index detector and a two-column (Shodex KD-804 and KD-802) sequence. High-performance liquid chromatography-grade *N,N*-dimethylformamide with 10 mM LiBr was used as the eluent. The experiment was conducted at a flow rate of 1.0 mL min⁻¹ at 40 °C. Molecular mass calibration was performed

using Fluka PEG/poly(ethylene oxide) standard ReadyCal sets (Sigma-Aldrich Japan G. K., Tokyo, Japan). The standard and samples were completely dissolved in the eluent and filtered through a 0.45 μm polytetrafluoroethylene syringe filter (ADVENTEC) before injection.

Thermal Properties of CGL. TMA was conducted to determine the glass transition temperature (T_g) and viscous thermal flow temperature (T_f) of CGL. TMA was performed by using a TMA Q400 system (TA Instruments-Waters LLC, New Castle, DE, USA) at a nitrogen flow rate of 100 mL min^{-1} . The vacuum-dried CGL sample (approximately 6 mg) was loaded on a platinum pan, and a flat aluminum lid was gently placed on top of the sample. The CGL sample was heated from room temperature to 200 $^{\circ}\text{C}$ at a heating rate of 5 $^{\circ}\text{C min}^{-1}$ under an applied load of 0.05 N. T_g and T_f were determined at the first and second transition points, respectively, in the TMA profiles by using the TA universal analysis software.

TGA was used to determine the decomposition starting temperature (T_{dst}) and maximum decomposition temperature (T_{dmax}) of the CGL. TGA was performed using a TGA Q500 instrument (TA Instruments-Waters LLC, New Castle, DE, USA) at nitrogen flow rates of 60 and 40 mL min^{-1} for the sample and balance chambers, respectively. The vacuum-dried CGL sample (approximately 7 mg) was initially heated to 105 $^{\circ}\text{C}$ at a rate of 10 $^{\circ}\text{C min}^{-1}$ and isothermally maintained for 20 min, followed by heating to 850 $^{\circ}\text{C}$ at a heating rate of 10 $^{\circ}\text{C min}^{-1}$. T_{dst} and T_{dmax} were estimated as the temperatures corresponding to 5 wt % and maximum weight losses, respectively, in the TGA profiles using the TA universal analysis software.

RESULTS AND DISCUSSION

Yields of Fractional Components. CGLs prepared at the reaction temperatures of 140, 150, and 160 $^{\circ}\text{C}$ are denoted CGL-140, CGL-150, and CGL-160, respectively. GLs prepared using PEG200 and MPEG-n4 at a reaction temperature of 140 $^{\circ}\text{C}$ in a previous study are labeled PEG200L-140 and MPEG-n4L-140, respectively.¹²

Figure 2 illustrates the yields of CGLs and the corresponding solid residues as a function of the solvolysis reaction time. The yield of the CGL fractions gradually increased with increasing reaction time, whereas that of the solid residues decreased accordingly. This indicates that the acid-catalyzed

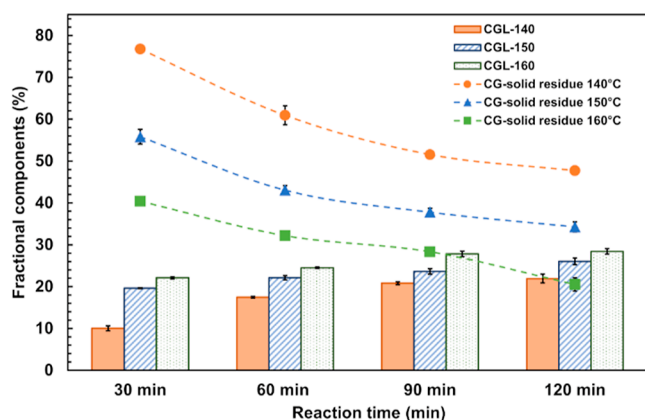


Figure 2. Yields of CGLs and solid residues as a function of the reaction time.

CG solvolysis of softwood proceeded with an increasing reaction time. The yields of CGL-140 for the reaction times of 30, 60, 90, and 120 min were 10.2, 17.7, 21.5, and 22.3%, respectively. The yield of CGL-140 showed smaller values than those of PEG200L-140 (25.8%) and MPEG-n4L-140 (24.8%) for a reaction time of 90 min.¹² Furthermore, the CGL yield was higher at higher reaction temperatures of 140, 150, and 160 $^{\circ}\text{C}$. At all reaction temperatures, the CGL yields increased up to 90 min and then plateaued. This trend was similar to those observed for the PEG and MPEG systems in previous studies.^{9,12} Therefore, a reaction time of 90 min was chosen as the solvolysis time for subsequent studies of the physical and chemical properties of CGL.

Table 1 lists the Klason- and acid-soluble lignin contents of CGLs and the corresponding solid residues of CGL-140, CGL-

Table 1. Klason and Acid-Soluble Lignin Contents of CGL and the Corresponding Solid Residues

	Klason lignin (%)	acid-soluble lignin (%)
CGL-140	81.5	0.87
CGL-150	78.3	0.90
CGL-160	79.8	1.05
CGL-140 solid residue	10.4	0.45
CGL-150 solid residue	6.4	0.54
CGL-160 solid residue	11.6	0.57

150, and CGL-160 for a reaction time of 90 min. Among CGL-140, CGL-150, and CGL-160, CGL-140 exhibited the highest Klason lignin content, whereas CGL-150 possessed the lowest. The Klason lignin content of CGL-160 was higher than that of CGL-150. The Klason lignin content of CGL might suggest the amount of CG incorporated into the lignin structure. The acid-soluble lignin content of CGL was higher at higher reaction temperatures. Yasuda et al. reported that acid-soluble lignin might be composed of low-molecular-weight degradation products and hydrophilic derivatives of lignin.¹⁹

Characterization of CGL. ATR-FTIR Spectroscopy. Figure 3a depicts the ATR-FTIR spectra of CG, which was used as the solvolysis reagent, MWL extracted from Japanese cedar wood meal, and CGL-140 for a reaction time of 90 min.¹⁷ The ATR-FTIR spectrum of MWL depicted typical characteristic lignin bands at 3400 (O–H stretching), 2937 (C–H stretching), 1594 (aromatic ring C=C–C stretching), 1510 (aromatic ring C=C–C stretching), 1462 (C–H deformation), 1269 (G-ring breathing with C=O stretching), 1140 (aromatic–aliphatic ether), and 1092 cm^{-1} (C–O deformation in secondary alcohol and ether).^{17,20} The ATR-FTIR spectrum of CG demonstrated absorption peaks at 2956 (methyl C–H stretching), 2925 and 2852 (methylene C–H stretching), and 856 cm^{-1} (CH_2 rocking), the fingerprint region.^{21–23} The ATR-FTIR spectrum of CGL-140 with a reaction time of 90 min comprised peaks similar to those observed in the MWL spectrum, suggesting that CGL exhibits a typical absorption due to lignin. The absorption peaks corresponding to C–H stretching in the CGL spectrum were detected at 2954, 2931, and 2860 cm^{-1} , and the peak corresponding to CH_2 rocking was observed at 856 cm^{-1} , suggesting the incorporation of CG into the lignin-derived moiety.

The ATR-FTIR spectra in Figure 3b depict the effects of the reaction temperature of CGLs for a reaction time of 90 min. CGLs prepared at higher reaction temperatures demonstrated a higher absorption of C–H stretching (2800–3000 cm^{-1}).

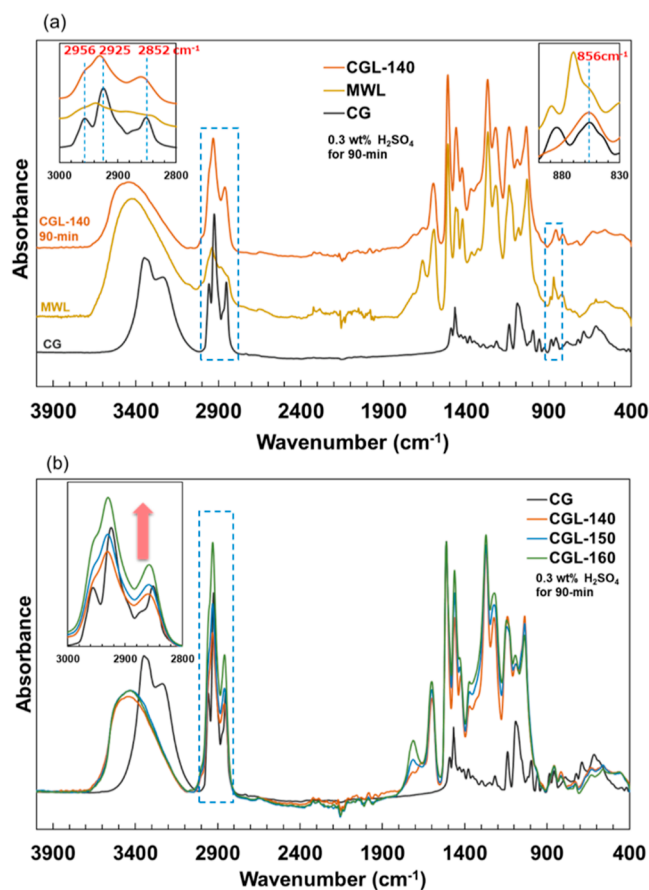


Figure 3. (a) ATR-FTIR spectra of CG, MWL, and CGL-140 for a reaction time of 90 min. (b) ATR-FTIR spectra of CG and CGLs as a function of the reaction temperature.

This suggests that the CGL sample prepared at a higher reaction temperature possesses a higher amount of introduced CG.

2D HSQC NMR Analysis. The 2D HSQC NMR spectra of CGLs, CG, and purified Sugi (Japanese cedar) MWL are depicted in Figure 4. The aliphatic subregion (δ_C/δ_H 10–38/0–2.6 ppm) in Figure 4a indicates the alkyl chain of CG, including the methyl group at the C_8 position, and the C_8 – H_8 correlation (CG_8) at δ_C/δ_H 14.0/0.8 ppm. Figure 4b presents the oxygenated aliphatic subregions (δ_C/δ_H 50–90/2.4–6.0 ppm) of CGLs, the methoxy groups of MWL ($-OCH_3$, δ_C/δ_H 55.6/3.7 ppm), and three types of interunit linkages. The HSQC NMR spectrum of MWL displays signals from the major lignin intermonomeric units.¹⁰ A strong signal of α -OH- β -O-4 (I) was observed in the MWL spectrum. However, this signal was not observed for CGL; however, clear intense signals of α -CG- β -O-4 (I') and substituted CG chains (CG_1 – CG_8) were detected. These NMR spectral data suggested that CG was introduced at the α -position of the β -O-4 bond. A proposed reaction mechanism is illustrated in Scheme 1. Furthermore, β -5 (II) and β - β (III) linkages were noted as the major intermonomeric linkage types in CGL. The aromatic subregions (δ_C/δ_H 105–130/6.0–8.0 ppm) in Figure 4c depict the guaiacyl nuclei (G_2 , G_3 , and G_6) of the lignin structure.

Figure 5 presents the signal ratio of CG and lignin methoxy groups (CG_8/Ome), which reflects the degree of CG introduction. The CG_8/Ome values of CGL-140, CGL-150, and CGL-160 for a reaction time of 90 min were 0.48, 0.53,

and 0.73, respectively. This result suggests that the amount of CG introduced is higher at higher reaction temperatures, which is in agreement with the ATR-FTIR spectral data (Figure 3b).

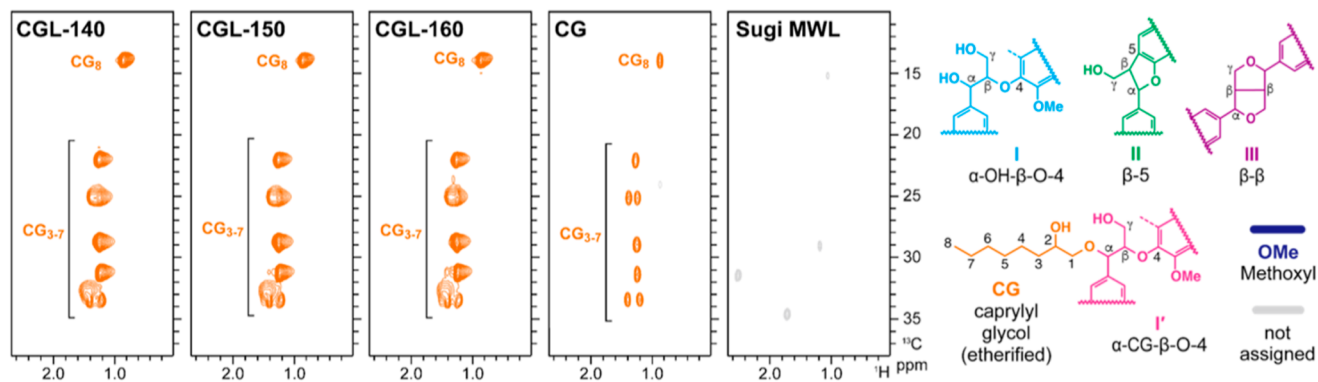
Figure 6 depicts the relative composition of the major interunit linkages (β -O-4, β -5, and β - β) based on the corresponding contour signal intensities (see Experimental Section). In CGL-140, the proportion of the β -O-4 linkage unit was 48% of the total major interunit linkages. A PEG200 solvolysis system of the same wood meal used in this study has been reported to contain 44% of the β -O-4 linkage,¹⁰ indicating that the reactivity of the CG solvolysis system is similar to that of the PEG200 system. Neiva et al. reported that ball-milled lignin extracted with a 90:10 v/v dioxane/water mixture from Norway spruce comprised 44% β -O-4 of total interunit linkages, and Rietzler et al. reported that the β -O-4 content of spruce bark lignin extracted by dioxane was 31 per 100 aromatic units.^{24,25} In general, the β -O-4 proportion indicates the degree of lignin degradation during solvolysis. At high reaction temperatures, the proportions of the α -CG- β -O-4 linkage were 19 and 18% in CGL-150 and CGL-160, respectively. Furthermore, the proportions of the β -5 linkage in CGL-140, CGL-150, and CGL-160 were 25, 10, and 8%, respectively. These results suggest that the breakdown of β -O-4 and β -5 linkages proceeds at high solvolysis reaction temperatures. In contrast, the β - β linkage is not affected by the solvolysis reaction regardless of the reaction temperature.

SEC Analysis. Table 2 lists the number-average molecular weight (M_n), weight-average molecular weight (M_w), polydispersity (PD), and thermal properties of CGLs. The molecular weight of CGLs prepared at higher reaction temperatures was lower, indicating the fragmentation of lignin macromolecules at high reaction temperatures. The profile of the SEC molecular weight distribution of CGL-140 demonstrated a shoulder peak in the high-molecular-weight region; however, this peak was weaker at higher solvolysis temperatures (Figure S1). In the previous MPEG solvolysis system, the M_w values were lower at reaction temperatures up to 150 °C; however, the value was slightly higher at 160 °C.¹² CGLs exhibited a lower molecular weight than that of PEG200L-140 and MPEG-n4L-140 (Table 2). These results indicate that the type of solvolysis reagent affects the molecular weight distribution of GLs.

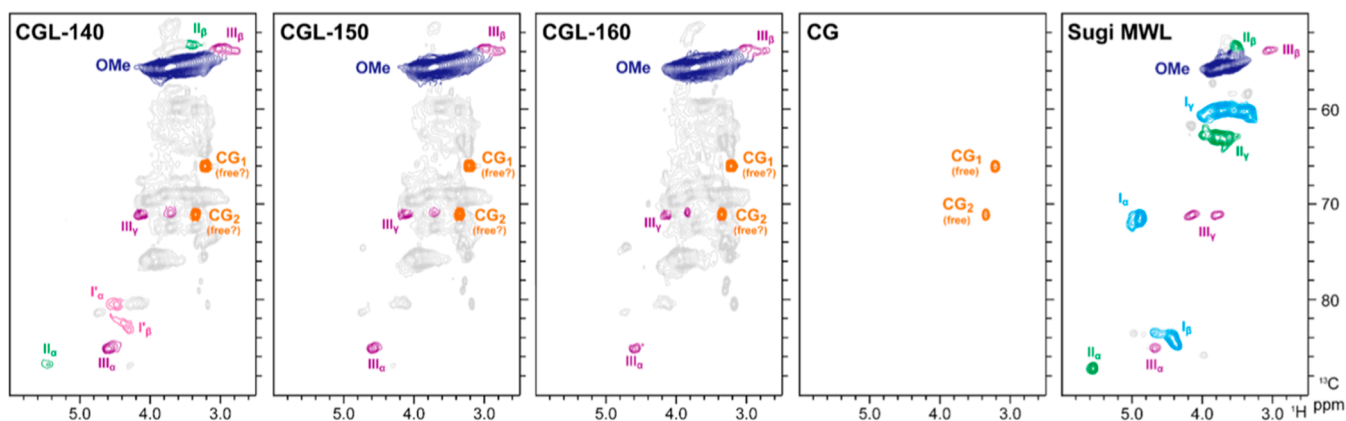
Thermomechanical Analysis. The change in the volume of CGLs was recorded as the distance moved by the probe with increasing temperature during TMA. Figure 7 depicts the TMA profiles of CGL-140, CGL-150, and CGL-160 for a reaction time of 90 min. In the CGL-140, CGL-150, and CGL-160 profiles, the first distinct inflection point corresponding to T_g was observed at 96, 95, and 89 °C, respectively. The second distinct inflection point corresponding to T_f due to the introduction of CG moieties to the lignin macromolecules was determined at 138, 155, and 134 °C for CGL-140, CGL-150, and CGL-160, respectively.

CGL possessed lower T_g and T_f values than those of the previously reported GLs, namely, PEG200L-140 and MPEG-n4L-140, which were prepared under the same conditions (140 °C and 90 min). Compared with the values of M_w of PEG200L-140 (M_w : 4130) and MPEG-n4L-140 (M_w : 3150), the lower M_w of CGL-140 (M_w : 2560) supported the result of the lower T_g and T_f values. The T_g value of lignin derivatives depends on their molecular weight, cross-linking structure, and hydrogen bonds.²⁶ Several studies have demonstrated the

(a) aliphatic subregion



(b) oxygenated aliphatic subregion



(c) aromatic subregion

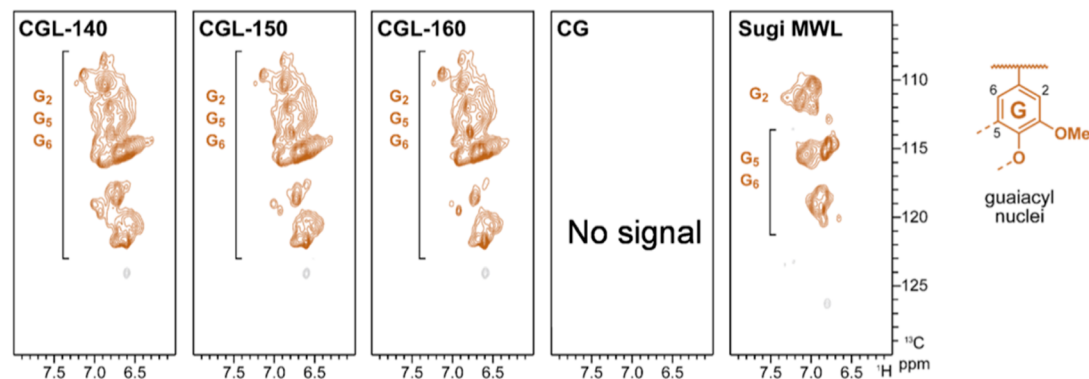
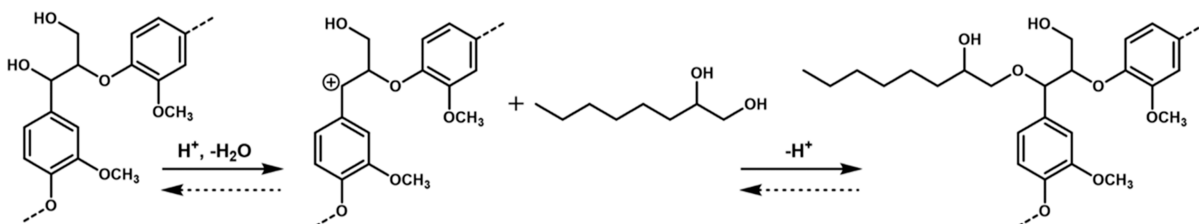


Figure 4. Two-dimensional HSQC NMR spectra of CGLs (CGL-140, CGL-150, and CGL-160), CG, and Sugi (Japanese cedar) MWL. (a) Aliphatic subregion, (b) oxygenated aliphatic subregion, and (c) aromatic subregion.

Scheme 1. Proposed Scheme for the Generation of CGL via Acid-Catalyzed CG Solvolysis of Softwood



enhancement of thermal properties by chemically modifying kraft lignin with alkyl chains.^{27,28} The esterification of the hydroxy group in lignin via the addition of long aliphatic chains reduced T_g because the ester substituent decreased the number

of hydrogen bonds in the lignin molecule, increasing the free volume in the molecule and consequently enhancing the mobility of the chains.²⁹ Suzuki and Iwata reported that the introduction of long-chain acyl groups ($C = 8$) into the

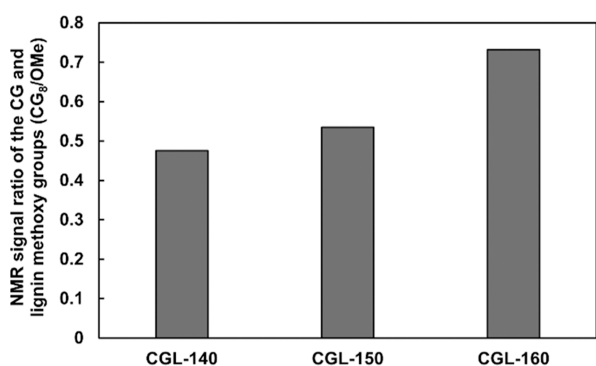


Figure 5. Signal ratio of CG contours per lignin methoxy group (CG_s/OMe) obtained via HSQC NMR analysis.

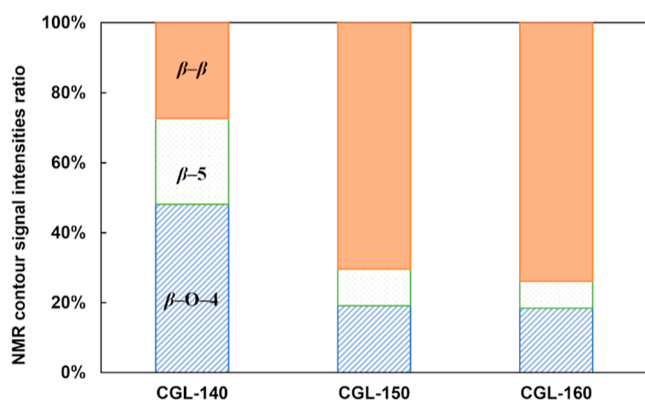


Figure 6. Proportion of major lignin linkage signals calculated using the normalized signal intensities of major oxygenated aliphatic subregion signals.

aliphatic hydroxy group of kraft lignin decreased the T_g value from 182 °C [kraft lignin substituted with short-chain acyl groups ($C = 2$)] to 132 °C.³⁰ This suggests that the thermal properties of GLs vary depending on the chemical structure of the solvolysis reagent, which was partially introduced into the lignin macromolecules during the solvolysis reaction.

Thermogravimetric Analysis. Figure S2 presents the TGA profiles of the CGLs. T_{dst} and T_{dmax} , which are the temperatures corresponding to 5% and maximum weight losses, respectively, were determined. The decomposition of lignin begins at 200–275 °C; the cleavage of β–β and C–C interunit bonds occurs at 273–350 °C; and the main degradation process occurs at approximately 400 °C.³¹ The T_{dst} values of CGL-140, CGL-150, and CGL-160 for a reaction time of 90 min were 256, 248, and 242 °C, respectively. These values provide information on the thermal stability of CGLs; i.e., the thermal stability of CGLs is lower at higher reaction temperatures. The derivative TG curves of CGLs demonstrated a small shoulder peak at 230–290 °C. This might be

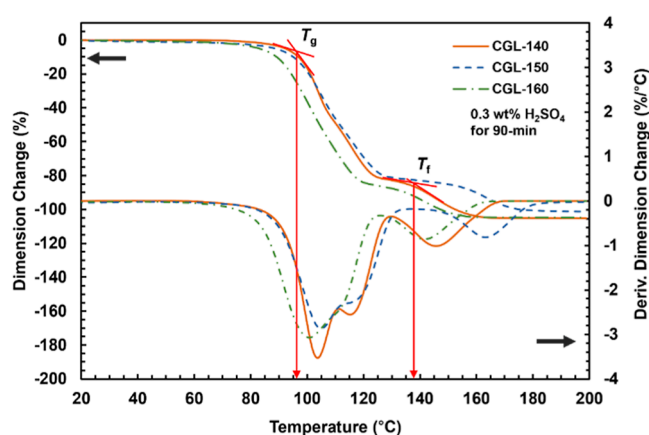


Figure 7. TMA profiles of CGL-140 (orange solid line), CGL-150 (blue dashed line), and CGL-160 (green chain line) for a reaction time of 90 min.

due to the degradation of the propanoid side chain, which was reported to occur at 230–260 °C.³¹ All CGLs exhibited similar T_{dmax} values of approximately 367–371 °C. No significant differences were observed in the T_{dmax} values between the types of GLs and solvolysis systems. The amount of char residues of CGL at 800 °C was 28–32%.

CONCLUSIONS

The acid-catalyzed solvolysis of softwood was performed using CG as the biobased solvolysis reagent. The CG solvolysis afforded the lignin derivatives (CGLs) with a yield of 21.5% at 140 °C and a reaction time of 90 min. CGL exhibited a lower molecular weight and lower T_g and T_f values in comparison to the previously reported GLs, such as PEG-lignin and MPEG-lignin. Two-dimensional HSQC NMR analysis suggested that CG was successfully incorporated into the lignin structure of CGL.

ASSOCIATED CONTENT

Supporting Information

The Supporting Information is available free of charge at <https://pubs.acs.org/doi/10.1021/acsomega.4c03278>.

SEC molecular weight distribution profiles of CGL-140, CGL-150, CGL-160, PEG200L-140, and MPEG-n4L-140 and TMA profiles of CGL-140, CGL-150, and CGL-160 (PDF)

AUTHOR INFORMATION

Corresponding Author

Tatsuhiko Yamada – *Life and Environmental Sciences, University of Tsukuba, Tsukuba, Ibaraki 305-8577, Japan; Center for Advanced Materials, Forestry and Forest Products*

Table 2. M_n , M_w , PD Values, and Thermal Properties of GLs

	M_n	M_w	PD (M_w/M_n)	T_g (°C)	T_f (°C)	T_{dst} (°C)	T_{dmax} (°C)	char residue at 800 °C (%)
CGL-140	1030	2560	2.5	96	138	256	371	30
CGL-150	940	2110	2.2	95	155	248	367	28
CGL-160	730	1840	2.5	89	134	242	367	32
PEG200L-140 ^a	1560	4130	2.6	116	160	261	368	36
MPEG-n4L-140 ^a	1260	3150	2.5	110	151	252	364	34

^a M_n , M_w , and PD values were cited from ref 12.

Research Institute, Tsukuba, Ibaraki 305-8687, Japan;
orcid.org/0000-0003-0585-2192; Email: yamadat@affrc.go.jp

Authors

Tomohiro Yamada – Life and Environmental Sciences, University of Tsukuba, Tsukuba, Ibaraki 305-8577, Japan; orcid.org/0009-0000-7714-8933

Yuki Tobimatsu – Research Institute for Sustainable Humansphere, Kyoto University, Uji, Kyoto 611-0011, Japan; orcid.org/0000-0002-7578-7392

Thi Thi Nge – Center for Advanced Materials, Forestry and Forest Products Research Institute, Tsukuba, Ibaraki 305-8687, Japan; orcid.org/0000-0001-7201-0222

Yusuke Matsumoto – Center for Advanced Materials, Forestry and Forest Products Research Institute, Tsukuba, Ibaraki 305-8687, Japan; orcid.org/0009-0001-8028-4896

Complete contact information is available at:

<https://pubs.acs.org/10.1021/acsomega.4c03278>

Author Contributions

The corresponding author, Tatsuhiko Yamada, conceived the idea for this study and designed the experiments. Tomohiro Yamada prepared the samples and conducted the ATR-FTIR spectroscopy, SEC, TMA, and TGA. Yuki Tobimatsu conducted the 2D HSQC NMR analysis. Thi Thi Nge and Yusuke Matsumoto contributed to the analysis of the samples and preparation of the manuscript with all authors.

Notes

The authors declare no competing financial interest.

ACKNOWLEDGMENTS

This work was supported by the Ministry of Agriculture, Forestry and Fisheries, Japan-commissioned project study on “Development of Glycol Lignin-Based High-Value-Added Materials,” grant no. J008722.

ABBREVIATIONS

GL, glycol lignin; CG, caprylyl glycol; CGL, caprylyl glycol lignin

REFERENCES

- (1) Kazzaz, A. E.; Fatehi, P. Technical lignin and its potential modification routes: A mini-review. *Ind. Crops Prod.* **2020**, *154*, 112732–112744.
- (2) Vishtal, A.; Kraslawski, A. Challenges in industrial applications of technical lignins. *BioResources* **2011**, *6* (3), 3547–3568.
- (3) Lora, J. H. Lignin: A Platform for Renewable Aromatic Polymeric Materials. In *Quality Living Through Chemurgy and Green Chemistry; Green Chemistry and Sustainable Technology*; Springer, 2002; pp 221–261..
- (4) Aronovsky, S. I.; Gortner, R. A. The cooking process, IX, pulping wood with alcohols and other organic reagents. *Ind. Eng. Chem. Res.* **1936**, *28* (11), 1270–1276.
- (5) Johansson, A.; Aaltonen, O.; Ylinen, P. Organosolv pulping — methods and pulp properties. *Biomass* **1987**, *13*, 45–65.
- (6) Jiménez, L.; de la Torre, M. J.; Maestre, F.; Ferrer, J. L.; Pérez, I. Organosolv pulping of wheat straw by use of phenol. *Bioresour. Technol.* **1997**, *60* (3), 199–205.
- (7) Jiménez, L.; Pérez, A.; De la Torre, M. J.; Rodríguez, A.; Angulo, V. Ethyleneglycol pulp from tagasaste. *Bioresour. Technol.* **2008**, *99* (7), 2170–2176.

(8) Li, Y.; Jia, H.; Ruxianguli, R.; Yin, H.; Zhang, Q. Extraction of lignin from wheat straw by catalysts in 1,4-butanediol medium under atmospheric pressure. *BioResources* **2014**, *10* (1), 1085–1098.

(9) Nge, T. T.; Takata, E.; Takahashi, S.; Yamada, T. Isolation and Thermal Characterization of Softwood-Derived Lignin with Thermal Flow Properties. *ACS Sustainable Chem. Eng.* **2016**, *4* (5), 2861–2868.

(10) Nge, T. T.; Tobimatsu, Y.; Takahashi, S.; Takata, E.; Yamamura, M.; Miyagawa, Y.; Ikeda, T.; Umezawa, T.; Yamada, T. Isolation and Characterization of Polyethylene Glycol (PEG)-Modified Glycol Lignin via PEG Solvolysis of Softwood Biomass in a Large-Scale Batch Reactor. *ACS Sustainable Chem. Eng.* **2018**, *6* (6), 7841–7848.

(11) Nge, T. T.; Yamada, T.; Tobimatsu, Y.; Yamamura, M.; Ishii, R.; Tanaike, O.; Ebina, T. Fractionation and Characterization of Glycol Lignins by Stepwise-pH Precipitation of Japanese Cedar/Poly(ethylene glycol) Solvolysis Liquor. *ACS Sustainable Chem. Eng.* **2021**, *9* (2), 756–764.

(12) Yamada, T.; Matsumoto, Y.; Nge, T. T.; Yamada, T. Acid-catalyzed solvolysis of softwood using polyethylene glycol monomethyl ether to produce functional lignin derivatives. *BioResources* **2023**, *18* (2), 3654–3665.

(13) Lee, E.; An, S.; Cho, S.; Yun, Y.; Han, J.; Hwang, Y. K.; Kim, H. K.; Lee, T. R. The influence of alkane chain length on the skin irritation potential of 1,2-alkanediols. *Int. J. Cosmet. Sci.* **2011**, *33*, 421–425.

(14) Johnson, W.; Bergfeld, W. F.; Belsito, D. V.; Hill, R. A.; Klaassen, C. D.; Liebler, D.; Marks, J. G.; Shank, R. C.; Slaga, T. J.; Snyder, P. W.; Andersen, F. A. Safety Assessment of 1,2-Glycols as Used in Cosmetics. *Int. J. Toxicol.* **2012**, *31*, 147–168.

(15) Bettenhausen, C. Symrise launches biobased caprylyl glycol. *C&EN Global Enterprise* **2022**, *100* (14), 11.

(16) Sluiter, A.; Hames, B.; Ruiz, R.; Scarlata, C.; Sluiter, J.; Templeton, D.; Crocker, D. *Determination of Structural Carbohydrates and Lignin in Biomass (NREL/TP-510-42618)*; LAP, National Renewable Energy Laboratory: Golden, CO, USA, 2008.

(17) Nge, T. T.; Tobimatsu, Y.; Yamamura, M.; Takahashi, S.; Takata, E.; Umezawa, T.; Yamada, T. Effect of heat treatment on the chemical structure and thermal properties of softwood-derived glycol lignin. *Molecules* **2020**, *25* (5), 1167–1181.

(18) Mansfield, S. D.; Kim, H.; Lu, F.; Ralph, J. Whole plant cell wall characterization using solution-state 2D NMR. *Nat. Protoc.* **2012**, *7*, 1579–1589.

(19) Yasuda, S.; Fukushima, K.; Kakehi, A. Formation and chemical structures of acid-soluble lignin I: sulfuric acid treatment time and acid-soluble lignin content of hardwood. *J. Wood Sci.* **2001**, *47*, 69–72.

(20) Faix, O. Fourier transform infrared spectroscopy. In *Springer Series in Wood Science, Methods in Lignin Chemistry*; Dence, C. W., Lin, S. Y., Eds.; Springer: Berlin, 1992; pp 83–110.

(21) Rohman, A.; Che Man, Y. B.; Ismail, A.; Hashim, P. Application of FTIR Spectroscopy for the Determination of Virgin Coconut Oil in Binary Mixtures with Olive Oil and Palm Oil. *J. Am. Oil Chem. Soc.* **2010**, *87*, 601–606.

(22) Guo, Y. C.; Cai, C.; Zhang, Y. H. Observation of conformational changes in ethylene glycol-water complexes by FTIR-ATR spectroscopy and computational studies. *AIP Adv.* **2018**, *8* (5), 055308.

(23) Kuroda, Y.; Kubo, M. CH₂ Rocking Vibrations of Polyethylene Glycols. *J. Polym. Sci.* **1957**, *26*, 323–328.

(24) Neiva, D. M.; Rencoret, J.; Marques, G.; Gutiérrez, A.; Gominho, J.; Pereira, H.; del Río, J. C. Lignin from tree barks: chemical structure and valorization. *ChemSusChem* **2020**, *13*, 4537–4547.

(25) Rietzler, B.; Karlsson, M.; Kwan, I.; Lawoko, M.; Ek, M. Fundamental Insights on the Physical and Chemical Properties of Organosolv Lignin from Norway Spruce Bark. *Biomacromolecules* **2022**, *23* (8), 3349–3358.

- (26) Alwadani, N. S.; Fatehi, P. Modification of Kraft Lignin with Dodecyl Glycidyl Ether. *ChemistryOpen* **2019**, *8*, 1258–1266.
- (27) Kim, S.; Oh, S.; Lee, J.; Ahn, N.; Roh, H.; Cho, J.; Chun, B.; Park, J. Effect of alkyl-chain-modified lignin in the PLA matrix. *Fibers Polym.* **2014**, *15*, 2458–2465.
- (28) Kim, S.; Park, J.; Lee, J.; Roh, H.; Jeong, D.; Choi, S.; Oh, S. Potential of a bio-disintegrable polymer blend using alkyl-chain-modified lignin. *Fibers Polym.* **2015**, *16*, 744–751.
- (29) Gordobil, O.; Herrera, R.; Llano-Ponte, R.; Labidi, J. Esterified organosolv lignin as hydrophobic agent for use on wood products. *Prog. Org. Coat.* **2017**, *103*, 143–151.
- (30) Suzuki, S.; Iwata, T. Selective substitution of long-acyl groups into alcohols of kraft lignin over transesterification using ionic liquid. *J. Wood Sci.* **2021**, *67*, 53.
- (31) Brebu, M.; Vasile, C. Thermal degradation of lignin - review. *Cellulose Chem. Technol.* **2010**, *44*, 353–363.